International Journal of Aquatic Science
ISSN: 2008-8019
Vol 12, Issue 03, 2021

Thermohydraulic Performance Of Modified Ground Heat Exchanger For Different Working Fluids–Numerical Approach

Aashish Sharma[1], Ravindra D. Jilte[2]

[1,2]*School of Mechanical Engineering, Lovely Professional University, Punjab, India, 144411*

Abstract: To keep pace with advancements, we also need the energy to keep on running the system. Sustainable development has now become an integral part of development and thus renewable energy is getting the attention that was required for a long. The Ground Source Heat Pump (GSHP) is a passive energy system that can be installed in buildings to reduce the overall HVAC load. A novel pipe design is used to increase the overall heat transfer thus leading to a high heat transfer rate. The novel spirally corrugated pipe design is then tested for different working fluids numerically. The results show that spirally corrugated pipe receives higher temperature drop as compared to the plain pipe. A significant pressure drop is also observed for the spirally corrugated pipe. In cooling mode, a COP of 5.02 and 4.42 is observed for the spirally corrugated pipe and plain pipe respectively. The most economic and the most efficient combination are found.

Keywords: Ground Heat Exchangers, Spirally Corrugated Pipe, GSHP, Heat Transfer

1. INTRODUCTION

Energy is the primary source for the development of a country. Especially in countries like India, the continuous power supply is one of the biggest challenges. The scenario of energy consumption has been increasing in a few years as the population and the economy are increasing. Currently, our primary fuel for power generation is coal, which is a fossil fuel, which causes pollution and global warming. Out of total energy generation, the infrastructure sector alone consumes almost 40% of total generated energy, and a further rise up to 76% is estimated by the year 2040 [1]. A significant portion of energy consumption is for maintaining thermal comfort within a building.

Renewable energy technology can reduce net energy consumption. There are active and passive technologies for doing this. Ground Source Heat Pump (GSHP) is one of them. They have applicability in a variety of buildings and are most appropriate to reduce environmental impacts [2]. A thorough review of GSHP is done by many researchers [3]–[6]. Ground Heat Exchanger (GHE) is the critical component of a GSHP. This fluid either absorbs or releases heat from the ground, depending on the operating condition. GSHP system has been growing continuously, with a range of 10 to 30% in the past few decades [7].

The operating principle of a GHE is straightforward. Since the ground temperature, after a certain depth, does not vary much and remains relatively constant

throughout the year. For a shallow GHE, the ground temperature is found to be almost constant at a depth of 1 m [2]. Although the temperature varies as per the geographical location. The performance of GSHP depends on its GHE, which can be arranged vertically or horizontally with different pipe layouts [8] as in Figure 1. There are a variety of basic pipe loop systems [6]. The primary hurdle is the high installation cost associated with the digging of a well or borehole [9]. Therefore, the horizontal-GSHP becomes vital due to low installation cost as only a trench of 1-2 m deep is required. However, the large area requirement for installing pipe loops is not cost-effective. In most of the studies, water or water-antifreeze mixture is used as working fluid in GHE [10-12].

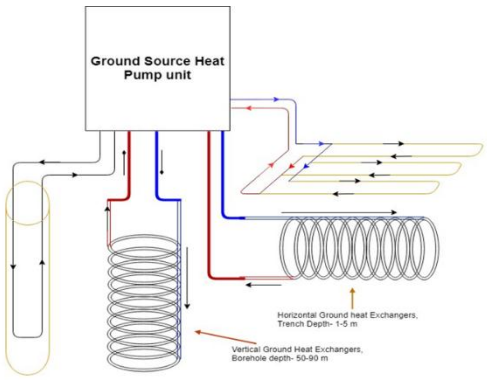

Figure 1: Different configurations of GHE.

Working fluid is also one of the primary components of a GHE and it is directly related to the performance of GHE. Various other working fluids have been tested for heat exchangers and have performed well in all parameters. Kumar et. al. [13] experimentally evaluated the thermohydraulic performance of Al2O3- water-based nanofluid. An increase in performance was observed with an increase in particle concentration. A low concentration of particles resulted in a low-pressure drop. Diglio et. al. [14] conducted a numerical study to evaluate the best low nanoparticle concentration (0.1-1%). A high concentration of nanoparticles resulted in a 3.8% rise in performance when compared to base working fluid i.e., water. Massimo et. al. [15] observed the behavior of nanofluid to be similar to that of single-phase fluid. Empirical relations were also formulated to evaluate the optimal particle loading. Effective thermal conductivity, Nusselt number, and viscosity results of various experimental and analytical studies have been presented by Huminic et. al. [16] in their review. Also, microencapsulated phase change material slurry (MPCMs) has been studied as heat transfer fluid by few researchers. Microencapsulation means when tiny particles of phase change material (PCM) are encapsulated in capsules. Due to the encapsulation of PCM, handling it becomes simple. For manufacturing MPCM, if the particle size is less than 100μm then the chemical process is used otherwise the physical process is used. Fabrication and characterization of MPCMs have been reviewed by Zhao et. al. [17]. Governing equations for heat transfer in MPCMs for circular duct were formulated by Charunyakorn et. al. [18]. Numerical analysis showed 2-4 times high heat flux in MPCMs as compared to single-phase working fluid. Various materials used and heat transfer studies of MPCMs by various researchers were reviewed by Delgado et. al. [19]. Due to its high thermal performance as compared to other single-phase fluids, MPCMs are one of the better options for heat exchanger application. MPCMs behave as Newtonian fluid at higher concentrations of up to 10.6% [20]. Jessica et. al. [21] have summarized the types, methods, and techniques of MPCMs and the detail of thermal properties can be found in their article. The latent heat of fusion of PCM enhances heat carrying capacity when its phase changes. Also, MPCMs have shown high pumping durability by showing resistance towards shearing due to pumping [22].

Also, a comparison for two different pipe geometries is done (Figure 2). A novel six-start spirally corrugated pipe has been compared to the plain smooth round pipe. The spirally corrugated pipes have shown good thermal enhancement characteristics [23], [24]. The thermohydraulic performance of various multi-start corrugated tubes can be found in this paper [25]. The effect of pitch and depth were analyzed by Jin et al. and they developed a relationship among them [26].

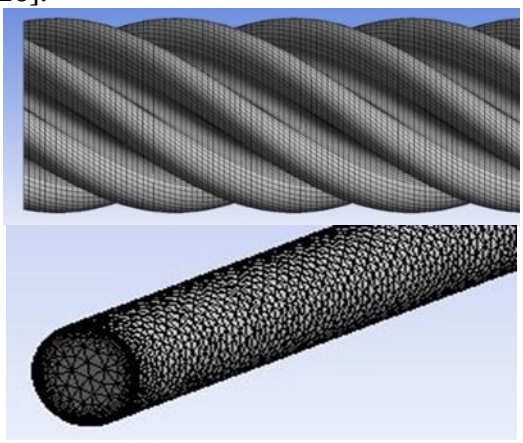

Figure 2: Novel spirally corrugated pipe (left) and plain smooth pipe (right) mesh.

Table 1: Properties of working fluids

	Mass/ volume Fraction (%)	**Density (kg/m^3)**	**Viscocity (mPa-s)**	**Effective Thermal Conductivity ($W/m\text{-}^0C$)**	**Specific Heat (J/Kg-K)**
Water	-	998.2	1.003	0.6	4182
MPCM Slurry CT02 [1]	6	982.4	1.76	0.589	1700
Al_2O_3 – water [2]	0.6	1068.99	1.89	0.451	3485.30

In this research, an effort has been made to reduce the overall size of GHE by improving its thermal performance. Since the working fluid has the most influence over thermal performance, three different working fluids, i.e., water, nanofluid (Al¬2O3), and microencapsulated phase change material (MPCM) slurry are studied numerically. Properties of fluids are given in Table 1.

2. NUMERICAL MODELLING AND VALIDATION:

A pipe length of 1 m was considered for this study. The pipe geometry was created using Creo parametric. Computational fluid dynamic (CFD) analysis was done using Ansys workbench as it is the most reliable and accurate software package available. The tetrahedral mesh was generated with the help of Fluent (Fig. 2). The standard k-ε turbulence and k-ω turbulence model were tested and the difference in outlet temperature was less than the order of 10-4. Thus, the standard k-ε turbulence model was selected along with scalable wall

functions (these shows better results when the flow is also rotating). Details of various parameters for the numerical model are given in Table 2. A simple method was used for numerical simulation. All the residuals are set to an order of 1e-06. Convergence was observed when the outlet temperature of the pipe stabilizes

Table 2: Parameters considered for the numerical study.

Parameter	
Pipe Length	1 m
Depth of burial	1.5 m
Internal pipe diameter	0.0254 m
Thermal conductivity of the soil	1.41 W/mK
Thermal diffusivity of soil	0.0036 m^2/h
Thermal conductivity of water	0.567 W/mK
Thermal conductivity of HDPE pipe	0.38 W/mK
Specific heat of the water	3.9 KJ/Kg-^{0}C
Velocity	0.5 m/s

3. GOVERNING EQUATION:

3.1.Continuity equation:

$$\frac{\partial u_r}{\partial r}+\frac{u_r}{r}+\frac{1}{r}\frac{\partial u_\theta}{\partial \theta}+\frac{\partial u_x}{\partial x}=0 \qquad (1)$$

3.2.Momentum equation r component:

$$\rho\left(u_r\frac{\partial u_r}{\partial r}+\frac{u_\theta}{r}\frac{\partial u_r}{\partial \theta}-\frac{u_\theta^2}{r}+u_x\frac{u_r}{x}\right)=-\frac{\partial P}{\partial r}+\mu\left(\frac{\partial^2 u_r}{\partial r^2}+\frac{1}{r}\frac{\partial u_r}{\partial r}-\frac{u_r}{r^2}+\frac{1}{r^2}\frac{\partial^2 u_r}{\partial \theta^2}-\frac{2}{r^2}\frac{\partial u_\theta}{\partial \theta}+\frac{\partial^2 u_r}{\partial x^2}\right) \textbf{(2)}$$

3.3.Momentum equation component:

$$\rho\left(u_r\frac{\partial u_\theta}{\partial r}+\frac{u_\theta}{r}\frac{\partial u_\theta}{\partial \theta}+\frac{u_r u_\theta}{r}+u_x\frac{\partial u_\theta}{\partial x}\right)=-\frac{1}{r}\frac{\partial P}{\partial \theta}+\mu\left(\frac{\partial^2 u_\theta}{\partial r^2}+\frac{1}{r}\frac{\partial u_\theta}{\partial r}-\frac{u_\theta}{r^2}+\frac{1}{r^2}\frac{\partial^2 u_\theta}{\partial \theta^2}+\frac{2}{r^2}\frac{\partial u_r}{\partial \theta}+\frac{\partial^2 u_\theta}{\partial x^2}\right) \textbf{(3)}$$

3.4.Momentum equation x component:

$$\rho\left(u_r\frac{\partial u_x}{\partial r}+\frac{u_\theta}{r}\frac{\partial u_x}{\partial \theta}+u_x\frac{\partial u_\theta}{\partial x}\right)=-\frac{\partial P}{\partial \theta}+\mu\left(\frac{\partial^2 u_x}{\partial r^2}+\frac{1}{r}\frac{\partial u_x}{\partial r}+\frac{1}{r^2}\frac{\partial^2 u_x}{\partial \theta^2}+\frac{\partial^2 u_x}{\partial x^2}\right) \textbf{(4)}$$

3.5.Energy equation:

$$\rho c_p\left(u_r\frac{\partial T}{\partial r}+\frac{u_\theta}{r}\frac{\partial T}{\partial \theta}+u_x\frac{\partial T}{\partial x}\right)=k\left(\frac{1}{r}\frac{\partial}{\partial r}\left(r\frac{\partial T}{\partial r}\right)+\frac{1}{r^2}\frac{\partial^2 T}{\partial \theta^2}+\frac{\partial^2 T}{\partial x^2}\right) \qquad \textbf{(5)}$$

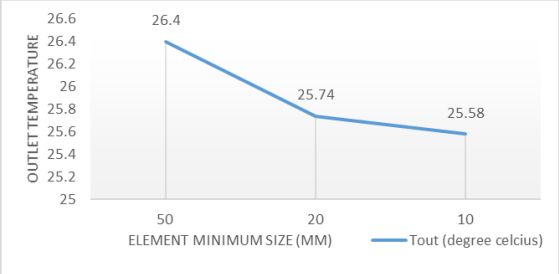

Figure 3: Grid Independence Test

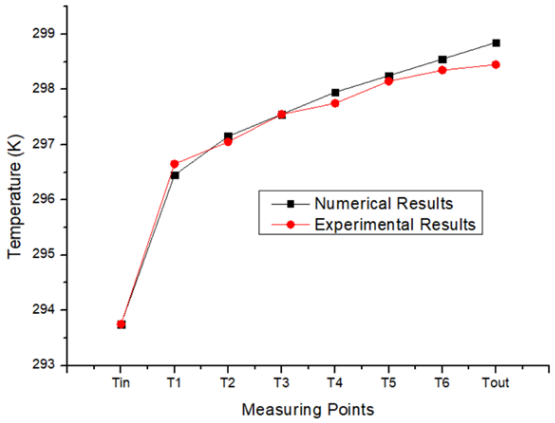

Figure 4: Temperature output as compared to the experimental results.

A Grid independence test was done to check the independence of results from the grid. The results are shown in Figure 3. Out of three meshing sizes, the medium was chosen to save computation time without losing accuracy. The numerical model was also experimentally validated by the experimental results. The errors were found to be well within the range of 5% (as shown in Figure 4).

4. RESULTS AND DISCUSSION:

At five different sections of the pipe (at every 0.25m), the temperature was calculated (Fig. 5). It can be seen from the contours that the fluid temperature decreases near to the surface. From the above comparison, the temperature drop is caused by the mixing of the flowing fluid because the turbulence is increased by this mixing. We can see the change in the temperature drop in the two pipes (Fig. 6). As the flow develops, it can be observed that turbulence helps increase the heat transfer rate. The difference in temperature drop is found to be 0.11 ℃.

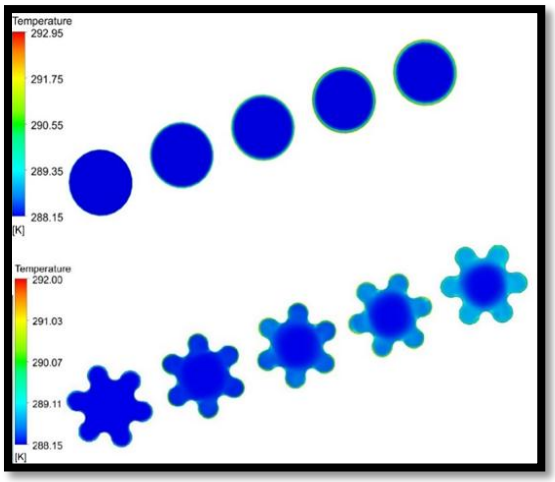

Figure 5: Temperature contours for both pipes

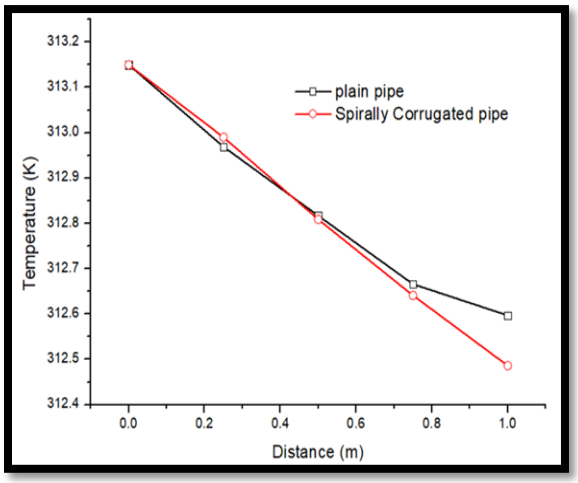

Figure 6: Temperature drop for both the pipes

4.1.Velocity distribution:

Velocity contours can be seen in Fig. 7. The velocity becomes maximum at the central axis because the directional velocity component increases as fluid flow along the spiral section of the pipe. Secondary flow distributions from various perspectives for better analysis of flow conditions are observed. At first 300 mm, the fluid particles near the wall are much faster than the other parts. A fluid flow is a developing flow profile that eventually transforms into a fully evolved periodic profile. While the fluid flows, the range of the accelerating fluid extends to the core of the spiral tube. The spiral tube produces additional swirling motion not found in smooth tubes.

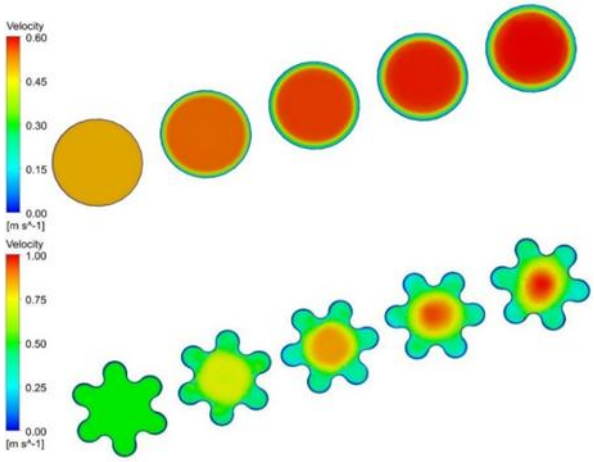

Figure 7: Velocity distribution in both pipes

4.2.Pressure drop:

Pressure drop refers to the amount of pressure head lost. This pressure drop is primarily due to friction. If the flow is laminar, these losses are less compared to turbulent flow.

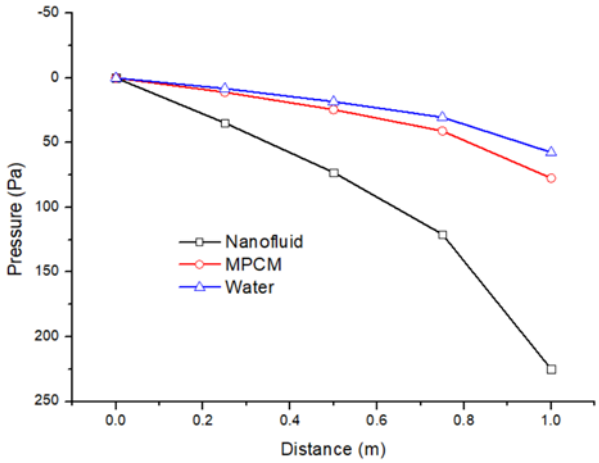

Figure 8: Pressure drop for Plain pipe.

4.3.Plain Pipe:

The calculations show that the pressure drop in the plain pipe for nanofluid is 3.9 times greater than the water. Also, the MPCM slurry faces significantly less pressure drop, i.e., 1.3 times that of water (Fig. 8).

4.4.Spirally Corrugated Pipe:

The pressure drop in the spirally corrugated pipe for nanofluid is 2.9 times greater than the water. The MPCM slurry faces significantly less pressure drop, i.e., 1.25 times that of water, which is almost similar to plain pipe (Figure 9).

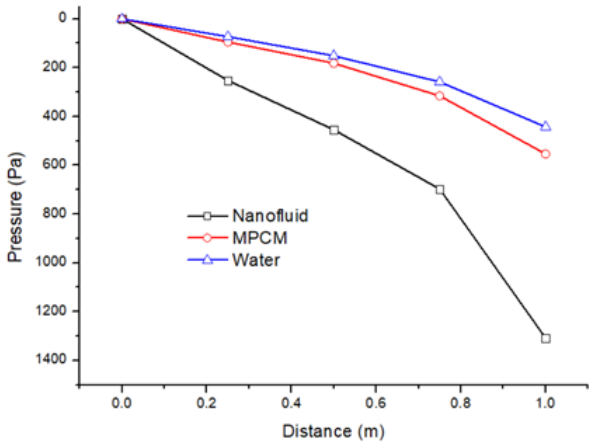

Figure 9: Pressure drop for Spirally Corrugated pipe.

Thus, it can be concluded that MPCM slurry is the best suited working fluid as its pressure drop is almost to that of water with a significant heat transfer coefficient. The primary reason for the high-pressure drop for nanofluid is the high particle concentration. A 6% concentration was chosen to compare it with a 6% MPCM concentration fluid. A comparison for pressure drop among both geometries, i.e., plain and spirally corrugated pipe, was made separately for each fluid. The pressure drop in the spiral pipe is 5.81, 7.15, and 7.7 times that of plain pipe, water, nanofluid and MPCM slurry as working fluid, respectively, as shown in Figures 27, 28, and 29.

4.5.Comparison of thermal performance in the spirally corrugated pipe for different working fluids in summer season

In Figure 10, we can see the variation of temperature drop for the plain pipe. We can observe that the maximum temperature drop is observed for MPCM slurry as working fluid. The difference in temperature drops of Nanofluid and water is 0.405 ^{0}C. Meaning, Nanofluid rejects more heat than the water in a plain pipe under the same conditions. Similarly, the temperature difference in the temperature drop of MPCM slurry and Nanofluid is 0.58^{0}C. Meaning, MPCM slurry rejects more heat than the Nanofluid in a plain pipe under the same conditions.

In Figure 11, the variation of temperature drop for the spirally corrugated pipe can be seen. The maximum temperature drop for MPCM slurry as working fluid is observed. The difference in temperature drops of Nanofluid and water is 0.549 ^{0}C. Meaning, Nanofluid rejects more heat than the water in a plain pipe under the same conditions. Similarly, the temperature difference in the temperature drops of MPCM slurry and Nanofluid is 0.647 ^{0}C. Meaning, MPCM slurry rejects more heat than the Nanofluid in spirally corrugated under the same conditions. If we compare the temperature drop of nanofluid among both the pipes, we can see that spirally corrugated tube outperforms by 0.155 ^{0}C. This can be seen in Figure 12; similarly, for MPCM slurry as working fluid, again spirally corrugated pipe gains 0.222^{0}C (Figure 13).

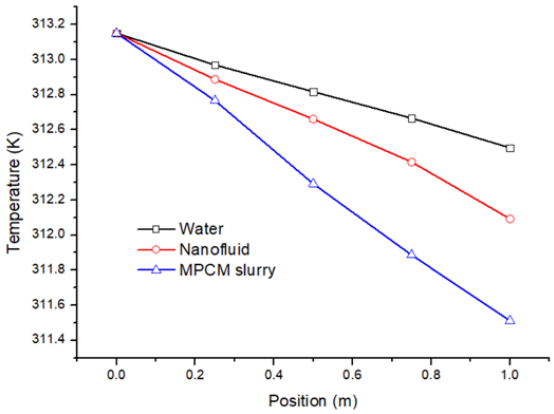

Figure 10: Temperature drop in the plain pipe for different working fluids.

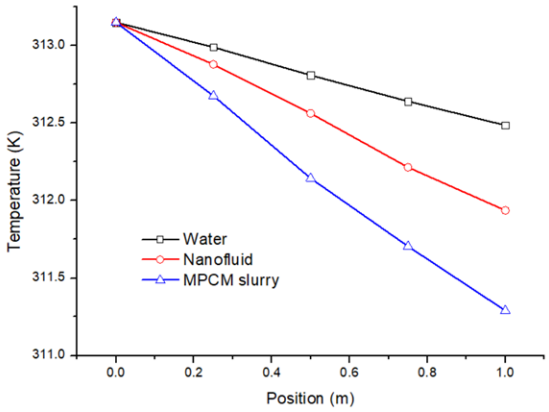

Figure 11: Temperature drop in the spirally corrugated pipe for different working fluids.

The COP of the system for the cooling can be seen in Table 2. If we compare the COP of water for plain pipe and spirally corrugated pipe, we can see a percentage increase of 3.4%. If we compare the COP of all three fluids for plain pipe, then we can see that again, COP of

MPCM slurry is the highest. The difference between COP of water and MPCM slurry is almost three times. Also, the difference between COP of water and Nanofluid is 1.18 times more or slightly higher than double.

Table 3: COP of fluids for the summer season.

Summer	Plain pipe	Spirally Corrugated pipe
Water	1.76	1.79
Al_2O_3 - water nanofluid	2.8	3.27
MPCM slurry	4.42	5.02

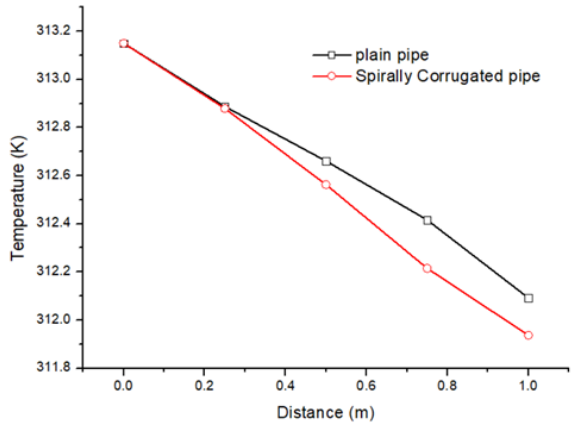

Figure 12: Temperature drop in both pipes for nanofluid as the working fluid.

Also, when we compare the Spirally corrugated pipe, we find that COP of MPCM slurry is 3.6 times higher when compared to the water. Also, the COP of nanofluid is found to be 1.65 times higher than that of water.
We can see that the difference in COP of nanofluid for the plain pipe and spirally corrugated pipe is 33%, and the difference in COP of MPCM slurry for the plain and spirally corrugated pipe is 27% high.

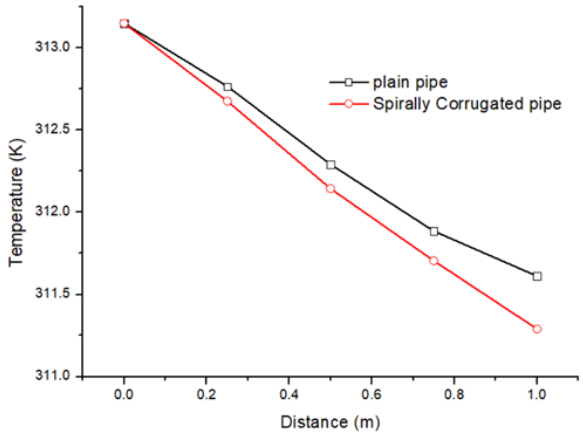

Figure 13: Temperature drop in both pipes for MPCM slurry as the working fluid.

5. CONCLUSION

- The simulations were carried out to evaluate cooling performance. The results show that there was an obvious temperature change of 0.11 0C when comparing the two pipe designs. Based on the results of the CFD simulation, the shape of the pipe can have a significant impact on the performance of the GHE system.
- Surface modifications are commonly used because they are very effective in improving heat transfer in heat exchangers. Spiral corrugations promote secondary recirculating flow by causing an axial velocity component. As the fluid passes, the vortex of the secondary flow and the curvature improves heat transfer as well as pressure loss.
- In terms of COP, it is seen that COP of the system having MPCM slurry as working fluid is the top-performing fluid. It gives a cooling COP of 5.02 when used in spirally corrugated pipe GHE compared to 4.42 for the plain pipe. Also, the difference in COP of nanofluid for spirally corrugated pipe and the plain pipe is 0.47 which is less when compared to pressure drop.

So, from this study, it can be concluded that the best combination for enhancing the overall thermohydraulic performance of a GHE will be the one using MPCM slurry with the plain pipe. It will help in reducing overall cost and it will be simple to manufacture.

6. REFERENCES

[1] B. K. S. K. V. S. R. Yogita Sharma, 'Energy Savings in a Building at Different Climatic Zones of India by Using Insulating Materials', Green Build. Sustain. Eng., pp. 167–78, 2018.

[2] N. Naili, I. Attar, M. Hazami, and A. Farhat, 'Experimental Analysis of Horizontal Ground Heat Exchanger for Northern Tunisia', J. Electron. Cool. Therm. Control, vol. 02, no. 03, pp. 44–51, 2012.

[3] L. Aresti, P. Christodoulides, and G. Florides, 'A review of the design aspects of ground heat exchangers', Renew. Sustain. Energy Rev., vol. 92, no. March, pp. 757–773, 2018.

[4] Florides, G., Kalogirou, S., 'Gound Heat Exchangers-A review', Ktisis, no. October, p. 8, 2004.

[5] N. Zhu, P. Hu, L. Xu, Z. Jiang, and F. Lei, 'Recent research and applications of ground source heat pump integrated with thermal energy storage systems: A review', Appl. Therm. Eng., vol. 71, no. 1, pp. 142–151, 2014.

[6] G. Florides and S. Kalogirou, 'Ground heat exchangers-A review of systems, models and applications', Renew. Energy, vol. 32, no. 15, pp. 2461–2478, 2007.

[7] S. Karytsas and H. Theodoropoulou, 'Public awareness and willingness to adopt ground source heat pumps for domestic heating and cooling', Renew. Sustain. Energy Rev., vol. 34, pp. 49–57, Jun. 2014.

[8] A. A. Serageldin, Y. Sakata, T. Katsura, and K. Nagano, 'Thermo-hydraulic performance of the U-tube borehole heat exchanger with a novel oval cross-section: Numerical approach', Energy Convers. Manag., vol. 177, pp. 406–415, 2018.

[9] S. Yoon, S. R. Lee, M. J. Kim, W. J. Kim, G. Y. Kim, and K. Kim, 'Evaluation of stainless steel pipe performance as a ground heat exchanger in ground-source heat-pump system', Energy, vol. 113, pp. 328–337, 2016.

[10] Y. Wu, G. Gan, A. Verhoef, P. L. Vidale, and R. G. Gonzalez, 'Experimental measurement and numerical simulation of horizontal-coupled slinky ground source heat exchangers', Appl. Therm. Eng., vol. 30, no. 16, pp. 2574–2583, 2010.

[11] P. F. Healy and V. I. Ugursal, ‘PERFORMANCE AND ECONOMIC FEASIBILITY OF GROUND SOURCE HEAT PUMPS IN COLD CLIMATE’, vol. 21, no. v, pp. 857–870, 1997.
[12] U. Camdali, M. Bulut, and N. Sozbir, ‘Numerical modeling of a ground source heat pump: The Bolu case’, Renew. Energy, vol. 83, no. June, pp. 352–361, 2015.
[13] P. C. Mukesh Kumar, J. Kumar, and S. Suresh, ‘Experimental investigation on convective heat transfer and friction factor in a helically coiled tube with Al2O3/water nanofluid’, J. Mech. Sci. Technol., vol. 27, no. 1, pp. 239–245, 2013.
[14] G. Diglio, C. Roselli, M. Sasso, and U. JawaliChannabasappa, ‘Borehole heat exchanger with nanofluids as heat carrier’, Geothermics, vol. 72, pp. 112–123, Mar. 2018.
[15] M. Corcione, M. Cianfrini, and A. Quintino, ‘Pumping Energy Saving Using Nanoparticle Suspensions as Heat Transfer Fluids’, J. Heat Transfer, vol. 134, no. 12, p. 121701, 2012.
[16] G. Huminic and A. Huminic, ‘Application of nanofluids in heat exchangers: A review’, Renewable and Sustainable Energy Reviews, vol. 16, no. 8. Pergamon, pp. 5625–5638, 01-Oct-2012.
[17] C. Y. Zhao and G. H. Zhang, ‘Review on microencapsulated phase change materials (MEPCMs): Fabrication, characterization and applications’, Renew. Sustain. Energy Rev., vol. 15, no. 8, pp. 3813–3832, 2011.
[18] P. Charunyakorn, S. Sengupta, and S. K. Roy, ‘Forced convection heat transfer in microencapsulated phase change material slurries: flow in circular ducts’, Int. J. Heat Mass Transf., vol. 34, no. 3, pp. 819–833, 1991.
[19] M. Delgado, A. Lázaro, J. Mazo, and B. Zalba, ‘Review on phase change material emulsions and microencapsulated phase change material slurries: Materials, heat transfer studies and applications’, Renew. Sustain. Energy Rev., vol. 16, no. 1, pp. 253–273, 2012.
[20] M. Kong, J. L. Alvarado, W. Terrell, and C. Thies, ‘Performance characteristics of microencapsulated phase change material slurry in a helically coiled tube’, Int. J. Heat Mass Transf., vol. 101, pp. 901–914, 2016.
[21] J. Giro-Paloma, M. Martínez, L. F. Cabeza, and A. I. Fernández, ‘Types, methods, techniques, and applications for microencapsulated phase change materials (MPCM): A review’, Renew. Sustain. Energy Rev., vol. 53, pp. 1059–1075, 2016.
[22] M. Kong, J. L. Alvarado, C. Thies, S. Morefield, and C. P. Marsh, ‘Field evaluation of microencapsulated phase change material slurry in ground source heat pump systems’, Energy, vol. 122, pp. 691–700, 2017.
[23] J. Qian et al., ‘Analysis of Fouling in Six-Start Spirally Corrugated Tubes Analysis of Fouling in Six-Start Spirally Corrugated Tubes’, Heat Transf. Eng., vol. 0, no. 0, pp. 1–16, 2019.
[24] Z. jiang Jin, F. qiang Chen, Z. xin Gao, X. fei Gao, and J. yuan Qian, ‘Effects of pitch and corrugation depth on heat transfer characteristics in six-start spirally corrugated tube’, Int. J. Heat Mass Transf., vol. 108, no. October, pp. 1011–1025, 2017.
[25] J. Qian, C. Yang, M. Chen, and Z. Jin, ‘Thermohydraulic performance evaluation of multi-start spirally corrugate d tub es’, Int. J. Heat Mass Transf., vol. 156, 2020.
[26] Z. jiang Jin, F. qiang Chen, Z. xin Gao, X. fei Gao, and J. yuan Qian, ‘Effects of pitch and corrugation depth on heat transfer characteristics in six-start spirally corrugated tube’, Int. J. Heat Mass Transf., vol. 108, pp. 1011–1025, 2017.
[27] N. A. Usri, W. H. Azmi, R. Mamat, K. A. Hamid, and G. Najafi, Heat Transfer Augmentation of Al2O3 Nanofluid in 60:40 Water to Ethylene Glycol Mixture, vol. 79. Elsevier B.V., 2015.

[28] T. Hymavathi & W. Sridhar, “Numerical Study of Flow and Heat Transfer of Casson Fluid Over an Exponentially Porous Stretching Surface in Presence of Thermal Radiation”, International Journal of Mechanical and Production Engineering Research and Development (IJMPERD) ,Vol. 8, Issue 4, pp, 1145-1154
[29] V Rambabu, J Ramarao & S Ravi Babu, “Enhancement of Heat transfer in Shell and Tube Heat Exchanger by Using Nano Fluid”, International Journal of Mechanical and Production Engineering Research and Development (IJMPERD) ,Vol. 7, Issue 5, pp, 191-198
[30] K. V. Chandra Sekhar, “Heat Transfer Analysis of Second Grade Fluid Over a Stretching Sheet Through Porous Medium Under the Influence of Chemical Reaction Parameter”, International Journal of Mechanical and Production Engineering Research and Development (IJMPERD) I,Vol. 8, Issue 1, pp, 605-612
[31] V. Murali Krishna, “Heat Transfer Enhancement by using CuO-Water Nanofluid in a Concentric Tube Heat Exchanger- an Experimental Study”, International Journal of Mechanical Engineering (IJME) , Vol. 6, Issue 1, pp; 11-20
[32] Pradumna Sharma & Suwarna Torgal, “Optimising Performance of Heat Exchanger Against Fouling”, International Journal of General Engineering and Technology (IJGET) , Vol. 6, Issue 4, pp; 41-46
[33] Hayder Kraidi Rashid Nasrawi, “Natural Convection Heat Transfer inside an Inclined Square Enclosure Filled with Al2o3 Nanofluid in Presence of Pair of Discrete Heat Flux Sources in Bottom Wall”, International Journal of Mechanical Engineering (IJME) ,Vol. 3, Issue 1, pp, 35-46